Inorg. Chem. **2007**, *46*, 11297–11307

The Presumption of Innocence? A DFT-Directed Verdict on Oxidized Amavadin and Vanadium Catecholate Complexes

K. R. Geethalakshmi, Mark P. Waller, and Michael Bühl*

Max-Planck-Institut für Kohlenforschung, Kaiser-Wilhelm-Platz 1, D-45470 Mülheim an der Ruhr, Germany

Received August 22, 2007

^{51}V NMR chemical shifts have been computed at the GIAO-B3LYP level for non-oxo vanadium(V) complexes related to oxidized amavadin, $[\Delta\text{-}V^{V}\{(S,S)\text{-hidpa}\}_2]^-$ (H_3hidpa = 2,2′-hydroxyiminodipropionic acid). According to model calculations, the unusual deshielding of the ^{51}V resonance is due to a combination of conventional substituent effects (e.g., oxo vs dihydroxo or alkoxy vs carboxylato ligands), rather than to a non-innocent nature of the hidpa ligand. For selected diastereomeric vanadium hidpa complexes, Born–Oppenheimer molecular dynamics simulations have been carried out to rationalize the observed differentiation of ^{51}V NMR chemical shifts. Strongly deshielded ^{51}V complexes that contain catecholate ligands do show significant disagreement between density functional theory (DFT)-computed chemical shifts and experiment. The possible cause for this deviation is indicated to result from ligand-to-metal charge transfer which can give rise to some open-shell character and temperature-dependent paramagnetic contributions. Electron-withdrawing groups at the catechol moiety tend to increase the corresponding transition energy, thereby reducing these contributions and limiting the non-innocence to the closed-shell ground-state wavefunction.

Introduction

^{51}V NMR spectroscopy is an important analytical tool for diamagnetic vanadium complexes.[1] ^{51}V is one of the most abundant natural isotopes with characteristics that are very favorable for NMR spectroscopy, affording a sensitive probe for the determination of the electronic and steric effects of the coordinating ligands. From the large body of data available, ranges of ^{51}V chemical shifts can be extracted that are characteristic for a given ligand environment and, to a lesser extent, for the oxidation state. Deviations from these "normal" chemical-shift ranges can suggest unusual electronic structures. For instance, unusually strong downfield shifts are observed for ^{51}V nuclei in vanadium(V) complexes containing catechol- or hydroxamate-based ligands (see Scheme 1), together with tridentate Schiff bases (or other stabilizing chelates). These downfield shifts can exceed 1000 ppm with respect to those of corresponding vanadates without these former ligands. This observation was first made by

Scheme 1

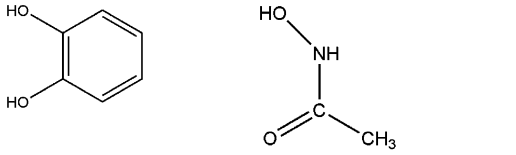

a. Catechol b. Acetohydroxamic acid

Pecoraro et al.[2] who labeled these ligands as "non-innocent" and who reported close relationships between ^{51}V chemical shifts and λ_{max} from low-energy electronic excitations in the near-IR spectra at around 900 nm. These excitations were assigned to ligand-to-metal charge transfer (LMCT). Contributions from resonance structures with open-shell character due to this LMCT have also been discussed[1b] (see Scheme 2).

Rehder et al.[3] in 2002 presented a series of biomimetic dioxovandium complexes with hydrazone tridentate ligands, some of which were also identified as non-innocent. Chakravorty et al.[4,5] characterized a series of vanadate esters

* To whom correspondence should be addressed. E-mail: buehl@mpi-muelheim.mpg.de. Fax: int. code + (0)208-306 2996.

(1) See for instance: (a) Rehder, D. In *Transition Metal Nuclear Magnetic Resonance*; Pregosin, P. S., Ed.; Elsevier: Amsterdam, 1991; pp 1−58. (b) Rehder, D.; Polenova, T.; Bühl, M. *Ann. Rep. NMR Spectrosc.* **2007**, *62*, 49−114.

(2) Cornman, C. R.; Colopas, G. J.; Hoeschele, J. D.; Kampf, J.; Pecoraro, V. L. *J. Am. Chem. Soc.* **1992**, *114*, 9925−9933.

(3) Maurya, M.; Khurana, S.; Zhang, W.; Rehder, D. *J. Chem. Soc., Perkin Trans. 2* **2002**, 3015−3023.

10.1021/ic701650y CCC: $37.00
Published on Web 11/22/2007

Scheme 2

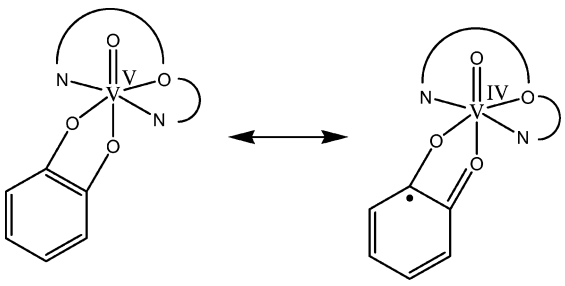

containing monoionized catechol ligands. Apparently, the proton remaining at one of the catecholate O atoms quenches much of the non-innocent behavior. The question of non-innocent ligands and their impact on ^{51}V NMR spectroscopy thus continues to be an interesting area of research and has been highlighted in a recent review.[1b]

According to Jørgensen, who introduced this term in chemistry in 1966, a ligand is innocent if it allows the unambiguous determination of the oxidation state of the central metal atom.[6] Non-innocent behavior of the ligands can be studied with a variety of experimental and theoretical techniques. For diamagnetic species, NMR spectroscopy is a convenient and sensitive probe into the electronic structure of transition-metal complexes, in particular if the central metal nucleus can be scrutinized, as exemplified by the aforementioned ^{51}V NMR spectroscopy. We were interested to what extent the computational tools of density functional theory (DFT), that had performed very well for ^{51}V chemical shifts of complexes with "normal" innocent ligands,[7] could be applied to reproduce and rationalize the unusual chemical shifts in the presence of non-innocent ligands. We now present a corresponding study of archetypical vanadium(V)−catechol complexes, calling special attention to their detailed electronic structure.

Oxidized amavadin is another species with an unusually high ^{51}V chemical shift, which, as had been speculated, could arise from non-innocent behavior of the ligands. Amavadin (**1**) is a vanadium(IV) complex with the composition [Δ-V^{IV}-{(*S*,*S*)-hidpa}$_2$]$^{2-}$, where H_3hidpa is 2,2′-hydroxyiminodipropionic acid. Amavadin is found in the fungal genus *Amanita* and has an unusual structure and metal−ligand bonding mode as shown in Figure 1. Since the isolation of this compound from *A. muscaria*[8] there have been discordant reports in the literature with respect to its structure and function.[9,10] Initially, a V=O species had been postulated,[11,12] whereas

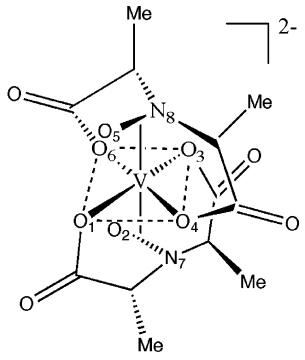

1.

Figure 1. Compound **1** (V^{IV}−hidpa)$_2$)$^{2-}$.

later studies indicated that amavadin is a non-oxo octacoordinated vanadium complex (see Figure 1).[13] Since amavadin is the only naturally occurring compound with such a structure, the apparent stability of this complex is very unusual.[14] The hydroxylamido moieties in the amavadin complexes have fascinated chemists for some time, and various model systems and spectroscopic characterizations have been carried out, including electron paramagnetic resonance (EPR) measurements.[15−18] Previous studies of vanadium hydroxylamido complexes have shown that the hydroxylamido ligand coordinates in a side-on manner as does the peroxo functionality.[19−21]

Amavadin and its derivatives are readily oxidized to afford diamagnetic vanadium(V) complexes, which are amenable to ^{51}V NMR spectroscopy. Oxidized amavadin [Δ-V^V{(*S*,*S*)-hidpa}$_2$]$^-$ and [Δ-V^V(hida)$_2$]$^-$ compounds (H_3hida = 2,2′-hydroxyiminodiacetic acid) showed single ^{51}V resonances at δ −281 and −263 ppm, respectively.[22] Further studies on model amavadin complexes obtained with (*R*,*S*)-H_3hidpa revealed, after oxidation, three signals at $\delta(^{51}V) = -250$, −270, and −280 ppm, due to the presence of three diastereomers.[23] In a recent study on the self-exchange electron transfer in amavadin-type complexes synthesized from the racemic hidpa ligand, Lenhardt et al. also reported three ^{51}V NMR signals for the oxidized form, at $\delta = -217$,

(4) Rath, S. P.; Rajak, K. K.; Chakravorty, A. *Inorg. Chem.* **1999**, *38*, 4376.
(5) Baruah, B.; Das, S.; Chakravorty, A. *Inorg. Chem.* **2002**, *41*, 4502−4508.
(6) Jørgensen, C. K. *Coord. Chem. Rev.* **1966**, *1*, 164.
(7) See for instance: (a) Bühl, M.; Hamprecht, F. A. *J. Comput. Chem.* **1998**, *119*, 113. (b) Bühl, M. *J. Inorg. Biochem.* **2000**, *80*, 137. (c) Bühl, M.; Schurhammer, R.; Imhof, P. *J. Am. Chem. Soc.* **2004**, *126*, 3310.
(8) Bayer, E.; Kneifel, H. *Z. Naturforsch.* **1972**, *27B*, 20.
(9) Nawi, M. A.; Reichel, T. L. *Inorg. Chim. Acta* **1987**, *136*, 33.
(10) Fraústo da Silva, J. J. R. *Chem. Speciation Bioavailability* **1989**, *1*, 139.
(11) Kneifel, H.; Bayer, E. *Angew. Chem.* **1973**, *85*, 542−543.
(12) Krauss, P.; Bayer, E.; Kneifel, H. *Z. Naturforsch., B: Anorg. Chem. Org. Chem* **1984**, *39b*, 829−832.
(13) Bayer, E.; Koch, E.; Anderegg, G. *Angew. Chem.* **1987**, *99*, 570−572.
(14) Bayer, E.; Koch, E.; Anderegg, G. *Angew. Chem., Int. Ed. Engl.* **1987**, *26*, 545−546.
(15) Carrondo, M. A. A. F. de C. T.; Duarte, M. T. L. S.; Pessoa, J. C.; Silva, J. A. L.; Fraústo da Silva, J. J. R.; Vaz, M. C. T. A.; Vilas-Boas, L. F. *J. Chem. Soc., Chem. Commun.* **1988**, 1158−1159.
(16) Fraústo da Silva, J. J. R.; Guedas Da Silva, M. F .C.; Da Silva, J. A. L. *Mol. Electrochem. Inorg. Bioinorg Organomet. Compds.* **1993**, 411−415.
(17) Remenyi, C.; Munzarova, M. L.; Kaupp, M. *J. Phys. Chem. B* **2005**, *109*, 4227−4233.
(18) Butler, A.; Clague, M. J.; Meister, G. *Chem. Rev.* **1994**, *94*, 625−638.
(19) Nuber, B.; Wriss, J. *Acta Crystallogr.* **1981**, *B37*, 947−948.
(20) Quilitzsch, U.; Wieghardt, K. *Z. Naturforsch.* **1979**, *34b*, 640−641.
(21) Meicheng, S.; Jing, L.; Zuohua, P.; Huadong, Z.; Youqi, T. *HuaXue XueBao* **1990**, *11*, 280−285.
(22) Armstrong, E. M.; Beddoes, R. L.; Calviou, L. J.; Charnock, J. M.; Collison, D.; Ertok, S. N.; Naismith, J. H.; Garner, C. D. *J. Am. Chem. Soc.* **1993**, *115*, 807.
(23) Smith, P. D.; Berry, R. E.; Harben, S. M.; Beddoes, R. L.; Helliwell, M.; Collison, D.; Garner, C. D. *J. Chem. Soc., Dalton Trans.* **1997**, 4509. See ref 8 within.

−234, and −252 ppm,[24] again due to the presence of three diastereomers. All these δ values display an unusually low shielding of the ^{51}V nucleus, given that hydroxylamine ligands, much like peroxo moieties, generally induce high field shifts, up to $\delta = -860$ ppm in oxo−vanadium complexes.[25,26] Since the low shielding in the oxidized amavadin derivatives could point to a non-innocent nature of the specific hydroxylamido ligands, we included the parent hida complex and selected stereoisomers of hidpa derivatives in the present study.

Computational Details

Stationary points were optimized with the *Gaussian 03* program[27] at the BP86/AE1 level, i.e., employing the exchange and correlation functionals of Becke[28] and Perdew,[29] respectively, together with a fine integration grid (75 radial shells with 302 angular points per shell), the augmented Wachters' basis[30] on V (8s7p4d, full contraction scheme 62111111/3311111/3111), and 6-31G* basis[31] on all other elements. For the amavadin-based model complexes the resolution of identity was used with fitting of the density, employing suitable auxiliary basis sets generated automatically in *Gaussian 03* (denoted RI-BP86). This and comparable DFT levels have proven quite successful for transition-metal compounds and are well suited for the description of structures, energies, barriers, etc.[32] The nature of the stationary points was verified by computations of the harmonic frequencies at that level. In selected cases, geometries were also optimized at the RI-BP86 level, as implemented in the *Turbomole* program,[33] using suitable auxiliary bases[34] and a medium-sized grid (m3).

For amavadin-derived species, Born−Oppenheimer molecular dynamics simulations (denoted BOMD) were performed at the RI-BP86/AE1 level, using the *ChemShell* program[35] for NVE ensembles at ca. 300 K for 0.001 ps, with a time step of 1 fs. In these simulations, the C−H distances were frozen with the SHAKE algorithm. Data and snapshot sampling was started after the first picosecond, which was taken for equilibration.

Magnetic shieldings were computed for equilibrium structures and for snapshots along the trajectories employing the B3LYP[36] hybrid functional, together with the AE1+ basis, i.e., AE1 augmented with diffuse functions on C, N, and O.[37] Snapshots were taken every 20 fs during 1−2 ps of the total runs. Chemical shifts are reported relative to $VOCl_3$, optimized or simulated at the same respective level (σ values are −2294 and −2320 ppm employing the BP86/AE1 and RI-BP86/AE1 geometries, respectively, and −2382 ppm for a BOMD simulation averaged over 1 ps).

In selected cases, magnetic shieldings were evaluated at the GIAO-B3LYP/AE1+ level in conjunction with the polarizable continuum model (PCM) of Tomasi and coworkers[38] (employing UFF radii and the parameters of water, both for geometries optimized in the gas phase and the continuum at the BP86/AE1 level.

Open-shell systems were described with the unrestricted formalism, and additional single-point energy computations were performed with the BHandH functional[39] as implemented in *Gaussian 03* and the AE1+ basis. The stability of the restricted DFT wavefunctions was tested with the method of Seeger and Pople.[40]

Results and Discussion

This section is organized as follows: First, oxidized amavadin is discussed (because it turns out that no non-innocent character needs to be ascribed to the ligands). Special attention is called to a possible assignment of stereoisomers when these are present. In the second part, catecholate complexes are investigated, with special emphasis on the details of their electronic structure that are responsible for the non-innocence manifested in the NMR spectra.

1. Oxidized Amavadin. Figure 2 shows the oxidized amavadin complex $[\Delta\text{-}V^{V}\{(S,S)\text{-hidpa}\}_2]^-$ (**2a**) and its hida analogue (**3**) as well as hypothetical species (**4**−**6**) with the same donor atoms in the first coordination sphere. These model species were constructed from **3** by deleting the appropriate atoms and saturating the dangling bonds with H atoms.

Geometries. Gas-phase- and PCM-optimized geometrical parameters for **2a** and selected stereoisomers as well as for

(24) Lenhardt, J.; Baruah, B.; Crans, D. C.; Johnson, M. D. *Chem. Commun.* **2006**, 4641.

(25) Paul, P. C.; Angus-Dunne, S. J.; Batchelor, R. J.; Einstein, F. W. B.; Tracey, A. S. *Can. J. Chem.* **1997**, *75*, 183.

(26) (a) Keramidas, A. D.; Miller, S. M.; Anderson, O. P.; Crans, D. C. *J. Am. Chem. Soc.* **1997**, *119*, 8901. (b) Tracey, A. S.; Jaswal, J. S. *J. Am. Chem. Soc.* **1992**, *114*, 3835.

(27) Frisch, M. J.; Trucks, G. W.; Schlegel, H. B.; Scuseria, G. E.; Robb, M. A.; Cheeseman, J. R.; Montgomery, J. A., Jr.; Vreven, T.; Kudin, K. N.; Burant, J. C.; Millam, J. M.; Iyengar, S. S.; Tomasi, J.; Barone, V.; Mennucci, B.; Cossi, M.; Scalmani, G.; Rega, N.; Petersson, G. A.; Nakatsuji, H.; Hada, M.; Ehara, M.; Toyota, K.; Fukuda, R.; Hasegawa, J.; Ishida, M.; Nakajima, T.; Honda, Y.; Kitao, O.; Nakai, H.; Klene, M.; Li, X.; Knox, J. E.; Hratchian, H. P.; Cross, J. B.; Adamo, C.; Jaramillo, J.; Gomperts, R.; Stratmann, R. E.; Yazyev, O.; Austin, A. J.; Cammi, R.; Pomelli, C.; Ochterski, J. W.; Ayala, P. Y.; Morokuma, K.; Voth, G. A.; Salvador, P.; Dannenberg, J. J.; Zakrzewski, V. G.; Dapprich, S.; Daniels, A. D.; Strain, M. C.; Farkas, O.; Malick, D. K.; Rabuck, A. D.; Raghavachari, K.; Foresman, J. B.; Ortiz, J. V.; Cui, Q.; Baboul, A. G.; Clifford, S.; Cioslowski, J.; Stefanov, B. B.; Liu, G.; Liashenko, A.; Piskorz, P.; Komaromi, I.; Martin, R. L.; Fox, D. J.; Keith, T.; Al-Laham, M. A.; Peng, C. Y.; Nanayakkara, A.; Challacombe, M.; Gill, P. M. W.; Johnson, B.; Chen, W.; Wong, M. W.; Gonzalez, C.; Pople, J. A. *Gaussian 03*; Gaussian, Inc.: Pittsburgh, PA, 2003.

(28) Becke, A. D. *Phys. Rev. A: At., Mol., Opt. Phys.* **1988**, *38*, 3098−3100.

(29) Perdew, J. P. *Phys. Rev. B: Condens. Matter Mater. Phys.* **1986**, *33*, 8822−8824. Perdew, J. P. *Phys. Rev. B: Condens. Matter Mater. Phys.* **1986**, *34*, 7406.

(30) (a) Wachters, A. J. H. *J. Chem. Phys.* **1970**, *52*, 1033−1036. (b) Hay, P. J. *J. Chem. Phys.* **1977**, *66*, 4377−4384.

(31) (a) Hehre, W. J.; Ditchfield, R.; Pople, J. A. *J. Chem. Phys.* **1972**, *56*, 2257−2261. (b) Hariharan, P. C.; Pople, J. A. *Theor. Chim. Acta* **1973**, *28*, 213−222. (c) Binning, R. C., Jr.; Curtiss, L. A. *J. Comput. Chem.* **1990**, *11*, 1206.

(32) See for instance: Koch, W.; Holthausen, M. C. *A Chemist's Guide to Density Functional Theory*; Wiley-VCH: Weinheim, Germany, 2000 and the extensive bibliography therein.

(33) Ahlrichs, R.; Bär, M.; Häser, M.; Korn, H.; Kölmel, M. *Chem. Phys. Lett.* **1989**, *154*, 165.

(34) (a) Eichkorn, K.; Treutler, O.; Öhm, H.; Häser, M.; Ahlrichs, R. *Chem. Phys. Lett.* **1995**, *240*, 283. (b) Eichkorn, K.; Weigend, F.; Treutler, O.; Ahlrichs, R. *Theor. Chem. Acc.* **1997**, *97*, 119.

(35) Sherwood, P.; deVries, A. H. *ChemShell—A Shell for Computational Chemistry*; CCLRC Daresbury Laboratory, 1999; see http://www.d-l.ac.uk.

(36) (a) Becke, A. D. *J. Chem. Phys.* **1993**, *98*, 5648. (b) Lee, C.; Yang, W.; Parr, R. G. *Phys. Rev. B: Condens. Matter Mater. Phys.* **1988**, *37*, 785−789.

(37) Clark, T.; Chandrasekhar, J.; Spitznagel, G. W.; Schleyer, P. v. R. *J. Comput. Chem.* **1983**, *4*, 294.

(38) As implemented in *Gaussian 03*: (a) Barone, V.; Cossi, M.; Tomasi, J. *J. Comput. Chem.* **1998**, *19*, 404−417. (b) Cossi, M.; Scalmani, G.; Rega, N.; Barone, V. *J. Chem. Phys.* **2002**, *117*, 43−54. (c) Cossi, M.; Crescenzi, O. *J. Chem. Phys.* **2003**, *19*, 8863−8872.

(39) Defined as $0.5E_X^{HF} + 0.5E_X^{LSDA} + E_C^{LYP}$; for the original formulation of the "half-and-half" hybrid functional see: Becke, A. D. *J. Chem. Phys.* **1993**, *98*, 1372.

(40) Seeger, R.; Pople, J. A. *J. Chem. Phys.* **1977**, *66*, 3045.

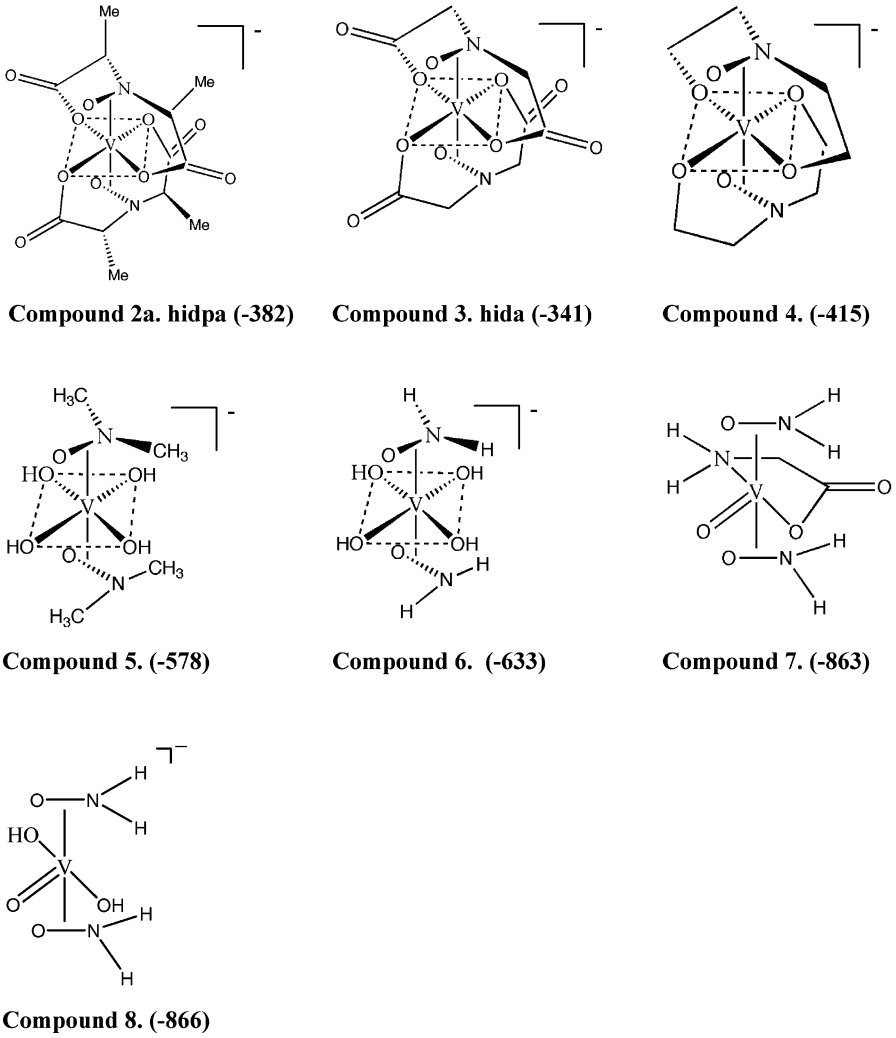

Figure 2. Oxidized amavadin **2a**, its parent **3**, and model complexes **4**−**6**, oxo-vanadium(V) hydroxylamido complex $[VO(NH_2O)_2Gly]$ (**7**), and model complex $[VO(NH_2O)_2(OH)_2]^-$ (**8**), together with computed gas-phase equilibrium ^{51}V chemical shifts (GIAO-B3LYP/AE1+ level, in parentheses).

Table 1. RI-BP86/AE1-Optimized Bond Lengths (Å) of the Diastereomeric Oxidized Amavadin Complexes $[\Delta\text{-}V^V(hidpa)_2]^-$ (**2**)

	2a	**2a**	**2a**	**2b**	**2c**	**2d**	**2e**	**2f**
	SS,SS *expt*[a]	SS,SS (PCM)	SS,SS	RR,RR	RR,SS	SR,RS	RS,SR	RS,RS
V−O_1	*1.993*	2.025	2.038	2.035	2.037	2.029	2.031	2.029
V−O_2	*1.923*	1.951	1.958	1.957	1.956	1.968	1.950	1.968
V−O_3	*1.959*	1.987	1.976	1.977	1.978	1.972	1.968	1.972
V−O_4	*1.977*	1.987	1.976	1.977	1.976	1.972	1.968	1.967
V−O_5	*1.940*	1.951	1.958	1.957	1.958	1.968	1.950	1.950
V−O_6	*1.972*	2.025	2.038	2.035	2.037	2.029	2.031	2.029
V−N_7	*2.018*	2.047	2.045	2.046	2.046	2.050	2.063	2.053
V−N_8	*1.999*	2.047	2.045	2.046	2.046	2.050	2.063	2.053

[a] Solid state, PPh_4^+ counterions, from ref 22; see Figure 1 for numbering of atoms.

Table 2. RI-BP86/AE1-Optimized Bond Lengths (Å) of the Oxidized Amavadin Model Complexes $[\Delta\text{-}V^V(hida)_2]^-$ (**3**) and for Selected Models Thereof

	3 *expt*[a]	**3**	**4**	**5**	**6**
V−O_1	*1.991*	2.041	2.036	2.037	2.109
V−O_2	*1.963*	1.961	1.953	1.953[b]	1.952
V−O_3	*1.955*	1.979	2.016	1.950	1.952
V−O_4	*1.920*	1.979	2.016	1.950	1.952
V−O_5	*1.936*	1.961	1.963	1.963[b]	1.952
V−O_6	*1.978*	2.041	2.036	2.036	2.109
V−N_7	*2.016*	2.038	2.040	2.040[b]	2.048
V−N_8	*2.028*	2.038	2.040	2.040[b]	2.048

[a] Solid state, PPh_4^+ counterions, from ref 22. [b] Fixed to the corresponding value of **4**.

3−**6** are collected in Tables 1 and 2, respectively, together with experimental data for **2a** and **3** in the solid state.[22] As expected, the different diastereomers of the oxidized amavadin (**2a**) have quite similar gas-phase-optimized bond lengths. The computed values for the all-S form **2a** and for **3** tend to be longer than those for the corresponding experimental ones, which may in part be due to packing effects in the solid, and may in part be related to the particular density functional employed.[41] Typically, distances are overestimated by a few picometers in the computations, with a maximum deviation of 0.046 Å for a V−N bond in **2a**.

For the discussion of substituent effects on the ^{51}V chemical shifts (see below), several model complexes **4**−**6** were constructed that preserve the general ligand environment of amavadin. Turning the carboxylate donors into alkoxy groups introduces only minor changes in the geo-

(41) Bühl, M.; Kabrede, H. *J. Chem. Theory Comput*. **2006**, *2*, 1282−1290.

metrical parameters (compare **3** and **4** in Table 2). Dissecting the tetradentate ligand backbone in **4** to afford **5** effectively leads to a dissociation of the N atoms from the metal (with fully optimized V−N distances of 2.978 Å in **5**). Apparently, the chelate is necessary to counteract the steric bulk of eight donor atoms about the metal. In order to evaluate substituent effects for the same ligand environment, we performed partial optimizations for **5**, in which the two V−N and V−O distances to the hydroxylamido moiety were fixed to their respective values in **4**. It is the data from these constrained optimizations that are included in Tables 1 and 2. Relative to the corresponding fully optimized minimum, this partially optimized structure of **5** is higher in energy by 23.7 kcal/mol (RI-BP86/AE1 level).[42]

Chemical Shifts. Equilibrium ^{51}V chemical shifts computed in the gas phase are included in Figure 2. For **2a** and **3**, the static values of $\delta = -382$ and -341 ppm, respectively, are considerably more shielded than the corresponding experimental numbers, $\delta = -281$ and -263 ppm, respectively, a frequent observation for this particular level of theory (see below for further results on **2a**−**h**). Figure 2 shows a typical oxovanadium(V) complex with two hydroxylamido ligands, [VO(NH_2O)$_2$Gly] (**7**, Gly = glycine anion).[26a] Even though some geometrical parameters observed for **7** in the solid state are not very well reproduced by the gas-phase optimization (see Table S1, Supporting Information), the computed ^{51}V chemical shift for **7**, $\delta = -863$ ppm, compares favorably to that of experiment, $\delta = -830$ ppm (aqueous solution value). Clearly, the substantial deshielding on going from **7** to **2a** is well captured by the computations.

Starting from **7**, model complex **8** was constructed by replacing the carboxylate and amine donors with hydroxy substituents. The vanadium(V) centers in both complexes are seven-coordinate in a pentagonal-bipyramidal geometry with the oxo ligand and an amino or hydroxy group in apical positions, and they contain two bidentate hydroxyamido ligands, one oxo ligand, and two monodentate N or O donors. The two hydroxylamido ligands are in an equatorial plane perpendicular to the V=O bond. Despite different overall charges and some variations in the metal−ligand bond distances (cf. Table S1, Supporting Information), the computed chemical shifts for **7** and **8** are remarkably similar (Figure 2). The latter is closely related to the amavadin model **6** in Figure 2, via the equation

$$\mathbf{6} \rightarrow \mathbf{8} + H_2O \qquad \Delta E = -7.8 \text{ kcal/mol (RI-BP86/AE1)} \quad (1)$$

On going from **8** to **6**, a substantial deshielding is computed for the ^{51}V nucleus, by $\Delta\delta = +233$ ppm. This large effect is difficult to analyze, because the mutual orientation of the ligands differs in both complexes. For instance, the X−V−X angle (where X denotes the midpoint of the side-on NO group) is 128° and 179° in **8** and **6**, respectively. In any event, it appears that the transition from a heptacoordinate oxo complex to an octacoordinate non-oxo species entails a large deshielding of the metal.

Replacing the hydroxylamido moieties in **6** with *N*,*N*′-dimethylhydroxylamido ligands (constraining the latter to prevent detachment) results in a further, slight downfield shift, $\Delta\delta = +55$ ppm (compare **6** and **5** in Figure 2). Closing the tetradentate ligand backbone by going from **5** to **4** produces another large deshielding, by $\Delta\delta = +163$ ppm. This rather large effect is mostly steric in nature, as the general electronic structure of both complexes should be very similar. One factor that arguably will contribute to this effect is the considerable elongation of the two V−O_3 and V−O_4 bonds by almost 0.07 Å in the course of this transformation (Table 2).

Mutating the alkoxy moieties in **4** into the carboxylate donors of the hidpa ligands in **3** produces a final, small downfield shift of $\Delta\delta = +74$ ppm. All these transformations just discussed have a deshielding effect on the central metal and add up to $\Delta\delta = +525$ ppm. Thus, the change in $\delta(^{51}V)$ between a typical oxovanadium complex **8** (or **7**) and the oxidized amavadin parent **3** can be broken down into a series of increments, the two most important of which stem from the difference between the oxo- and non-oxo complexes (i.e., an electronic effect) and from those between mono-/bidentate and tetradentate ligands (i.e., a steric effect). There is thus no need to invoke the non-innocent nature of the hidpa and related ligands to explain the observed unusual ^{51}V chemical shifts of oxidized amavadin and its derivatives.

Before turning to complexes with truly non-innocent ligands, we now discuss the ^{51}V chemical shifts of oxidized amavadin and its stereoisomers in more detail.

Stereoisomers. Natural amavadin **1** has been shown to consist of two diastereomers with the Δ-V{(*S*,*S*)-hidpa}$_2$ and Λ-V{(*S*,*S*)-hidpa}$_2$ configurations. The interconversion between forms is rapid in the native vanadium(IV) form but is kinetically hindered upon oxidation to the vanadium(V) species. Depending on the ligands employed and on their optical purity, synthetic amavadin derivatives can consist of complex equilibria between stereoisomers, which can give rise to multiple ^{51}V NMR signals in the oxidized forms. Depending on the source of the hidpa ligand, ^{51}V chemical shifts between $\delta = -217$ ppm and $\delta = -280$ ppm have been reported, a quite substantial variation for complexes with identical composition and connectivity that differ essentially in the stereochemistry at C atoms three bonds away from the metal. Even within the same probe, where experimental conditions are certainly exactly the same, variations of up to $\Delta\delta = 35$ ppm have been noted.

The stereoisomers considered in this study are shown schematically in Figure 3. They consist of the pairwise combinations of (S,S) and (R,R) forms, as well as pairs of the meso-(R,S) forms among themselves. Only Δ-isomers have been computed, as most of the corresponding Λ-isomers are implicitly included (e.g., Λ-V{(*S*,*S*)-hidpa}$_2$ and Δ-V{(*R*,*R*)-hidpa}$_2$ are enantiomeric pairs with identical energies and NMR parameters). In the study by Lenhardt et al.,[24] the racemic form of the hidpa ligand has been used to synthesize

(42) The stationary point for **6** turned out be a transition state; we discuss it here because it has the same orientations of the OR groups as in **2a.** The true minimum with an additional intramolecular H bridge is 0.65 kcal/mol lower in energy and it has a $\delta = -630$.

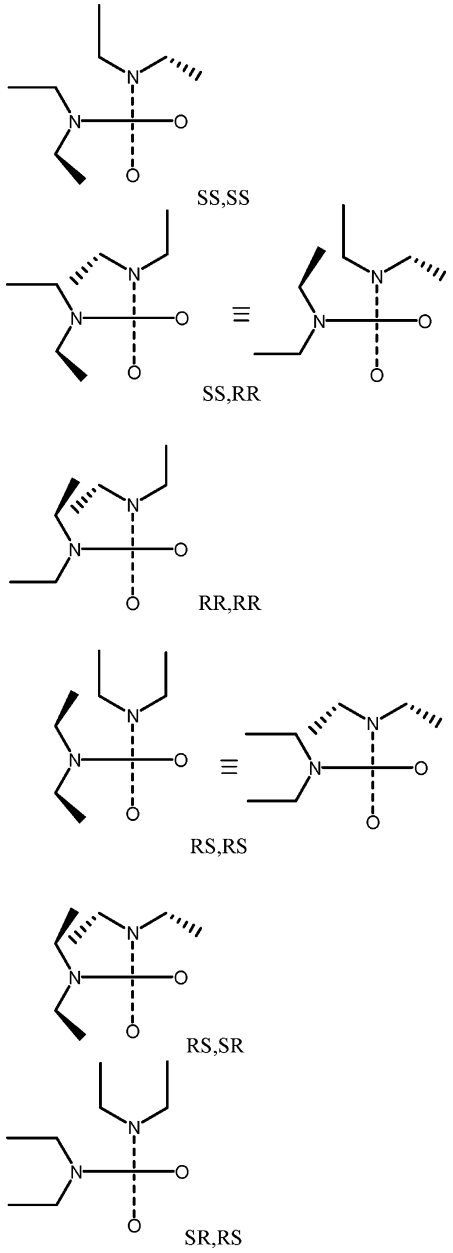

Figure 3. Amavadin diastereomers selected in this study (Δ forms); schematic views of the $(Me-C)_2-N-O$ fragments along the X−V−X axis (X = midpoint of NO groups).

the vanadium complexes in situ. This racemic form has been shown to consist of a mixture of (S,S)-, (R,R)-, and meso-(R,S)-isomers.[43] Thus, not only the pairwise combinations between each of these ligands are possible in the vanadium complexes but also mixed combinations such as (S,S) with (R,S). Such mixed forms have not been included in this study.

The equilibrium $\delta(^{51}V)$ values computed for a number of salient stereoisomers are all closely spaced around two values (ca. −380 and −350 ppm for complexes with asymmetric and meso ligands, respectively; see entry 2 in Table 3). No

Table 3. Relative Energies (in kcal/mol) and ^{51}V NMR Chemical Shifts δ (in ppm)[a] for Selected Amavadin Diastereomers

entry	isomer	**2a** SS,SS	**2b** RR,RR	**2c** RR,SS	**2d** SR,RS	**2e** RS,SR	**2f** RS,RS
1	E_{rel}, RI-BP86	0.00	0.17	0.10	0.4	11.37	5.96
	(B3LYP)[a]	0.00	0.47	0.19	1.79	11.77	6.91
2	δ_e (gas)[b]	−382	−381	−379	−357	−349	−354
3	δ (PCM//gas)[c]	−313	−311	−310	−302	−314	−308
4	δ (PCM//PCM)[d]	−353	−352	−349	−350		
5	δ_e (gas)[e]	−394	−393	−397	−382		
6	δ_{av} (BOMD)[f]	−355	−327	−340	−325		
7	expt δ[g]	−252	−217	−234			
8	expt δ[h]					−280/−270/−250	

[a] B3LYP/AE1+ level. [b] RI-BP86/AE1-optimized using *Gaussian 03*. [c] PCM single point on gas-phase-optimized geometries. [d] Geometries optimized with PCM. [e] RI-BP86/AE1 optimized using *Turbomole*. [f] Mean value over snapshots from BOMD trajectory. [g] Racemic ligand, ref 24. [h] meso-ligand, ref 23.

further differentiation is apparent between the isomers within each of the two groups upon inclusion of bulk solvent effects via a simple PCM approach, neither in terms of single-point computations on the gas-phase geometries (entry 3) nor upon relaxation in the continuum (entry 4). For selected isomers (**2a**−**d**), we have performed BOMD simulations in the gas phase and averaged the chemical shifts along the respective trajectories. This or similar procedures to model the thermal averaging of chemical shifts has recently been applied to other transition-metal complexes.[44] The BOMD simulations were done at the same level of theory as the *Gaussian 03* optimizations (RI-BP86/AE1), but with another program with a slightly different scheme for the numerical integration, resulting in slightly different equilibrium distances and chemical shifts (compare entries 2 and 5 in Table 3). Dynamical (thermal) averaging results in a noticeable general increase of the δ values, i.e., deshielding, and in a somewhat larger spread of the individual resonances (compare entries 5 and 6). For instance, while the equilibrium δ_e values of **2a** and **2b** are almost identical, the corresponding thermally averaged δ_{av} values differ by ca. 30 ppm. For the individual snapshots, fluctuations in the instantaneous magnetic shieldings are much larger than this value, but the running average over 50 or more such snapshots is well converged within this range, without showing a noticeable drift after 1 ps (see Figure S1, Supporting Information). Note that the computed deshielding due to thermal motion brings the δ_{av} values somewhat closer to experiment than the raw δ_e data.

As expected, this deshielding is related to an increase of the mean bond distances over the trajectories[45] with respect to the corresponding equilibrium values. On average, this elongation of the vanadium−ligand bonds amounts to 0.01 Å (see Table S2, Supporting Information).

For the complexes formed from the racemic ligand (**2a**−**c**), the computed sequence of the signals is in qualitative agreement with the observed pattern (assuming that the RR,-SS combination has double intensity), and the isomers are tentatively assigned correspondingly. For the complexes with

(43) (a) Koch, E.; Kneifel, H.; Bayer, E. *Z. Naturforsch* **1986**, *41b*, 359−362. (b) For a recent X-ray crystallography and NMR study see: Hubregtse, T.; Kooijman, H.; Spek, A. L.; Maschmeyer, T.; Sheldon, R. A.; Arends, I. W.; Hanafield, U. *J. Inorg. Biochem.* **2007**, *101*, 900−908.

(44) (a) Grigoleit, S.; Bühl, M. *Chem.—Eur. J.* **2004**, *10*, 5541−5552. (b) Bühl, M.; Grigoleit, S. *Organometallics* **2005**, *24*, 1516−1527.

(45) In each case, the mean values over the entire trajectories correspond closely to the mean values over the snapshots selected for the NMR computations.

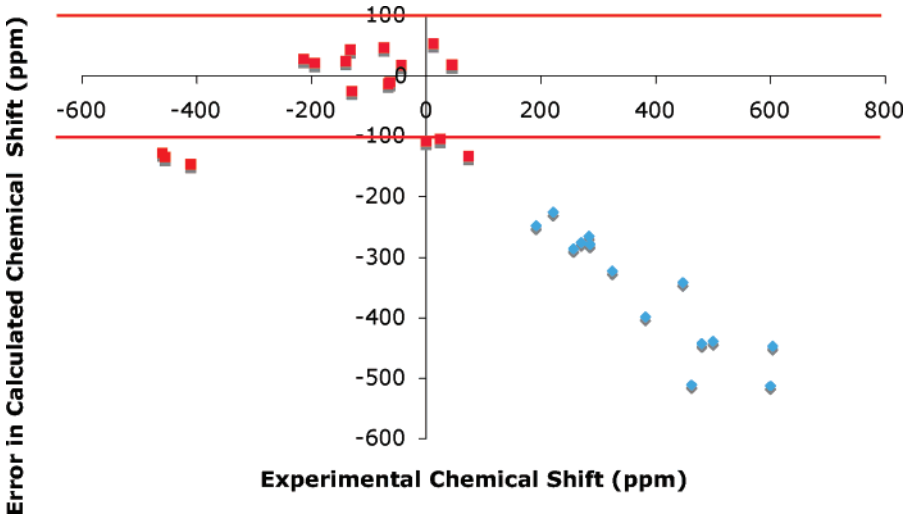

Figure 4. Scatter plot of the error in the GIAO-B3LYP-computed ^{51}V chemical shift (defined as $\delta_{calc} - \delta_{exp}$) vs experimental $\delta(^{51}V)$ values for 31 vanadium catecholate complexes collated from the literature (see Table S4, Supporting Information, for the full set of complexes). The upper and lower red lines are a visual indication of the empirically estimated error limit for DFT calculations of chemical shifts for vanadium complexes.

the meso ligand, MD simulations have been performed only for one representative (**2d**), because performing them for all possible components of the mixture would be a formidable task and because the confident assignment of experimental numbers to specific stereoisomers based on these results will probably be difficult.

2. Catechol Complexes. Chemical Shifts. A sizable number of vanadium catecholate and hydroxamate complexes are known,[2−5,46−53] many of them characterized both by X-ray crystallography and ^{51}V NMR spectroscopy. A selection of these (namely, a subset from refs 2−5 for which direct or indirect structural information in the solid was available; see Table S4 in the Supporting Information) was subjected to geometry optimizations starting from coordinates in the solid and to subsequent chemical-shift computations at the GIAO-B3LYP level. The results are plotted in Figure 4 as deviations from the experimental literature data. Two sets of data points can be discerned: complexes with observed ^{51}V resonances between ca. 0 and −400 ppm are reasonably well described computationally, with errors rarely exceeding ±100 ppm. This uncertainty is close to the degree of accuracy that has been achieved for other vanadate complexes at the same level of theory.[7] These data are clustered in the upper left of Figure 4 (with the error bar denoted by horizontal lines). For complexes with experimental ^{51}V chemical shifts above ca. 100 ppm, significantly larger errors are found, which in absolute size increase almost linearly with δ (data points in the lower right of Figure 4). In these cases, the observed strong deshielding of the metal is not reproduced, and the computed $\delta(^{51}V)$ values essentially remain below 100 ppm, even in cases where the experimental numbers reach 600 ppm.

Thus, high-frequency shifts of ^{51}V NMR resonances caused by potentially non-innocent ligands can only be reproduced with the current computational method up to a certain $\delta(^{51}V)$ value, ca. 100 ppm. Because the applied method imposes a strict closed-shell electronic structure on all complexes, it appears that up to this point no open-shell character due to charge transfer (viz., Scheme 2) needs to be invoked to explain the observed trends. The computed deshielding with respect to common vanadates rather arises from "normal" paramagnetic contributions due to the magnetic coupling of ground and excited states (represented by suitable occupied and virtual molecular orbitals (MOs) in the GIAO-DFT framework). These paramagnetic contributions are larger than those in common vanadates because the energetic separation of the coupled states is rather small, due to the presence of low-lying LMCT states. The particular importance of these states for the observed $\delta(^{51}V)$ values and correlations between the latter and the corresponding inverse excitation energies from visible and NIR transition wavelengths have been lucidly discussed in reference 2.[54]

The large GIAO-B3LYP errors for the exceptionally deshielded metal nuclei with $\delta(^{51}V)$ above 100 ppm can be either due to the severe underestimation of the paramagnetic contributions in the closed-shell wavefunctions or due to the mixing (or thermal population) of vanadium(IV)−semiquinone configurations into the electronic ground state (cf.

(46) Cooper, S. R.; Koh, Y. B.; Raymond, K. N. *J. Am. Chem. Soc.* **1982**, *104*, 5092.
(47) Kraft, B. J.; Coalter, N. L.; Nath, M.; Clark, A. E.; Siedle, A. R.; Huffman, H. C.; Zaleski, J. M. *Inorg. Chem.* **2003**, *42*, 1663.
(48) Kabanos, T. A.; White, A. J. P.; Williams, D. J.; Woollins, J. D. *Chem. Commun.* **1992**, 17.
(49) Simpson, C. L.; Pierpont, C. G. *Inorg. Chem.* **1992**, *31*, 4308.
(50) Hou, Z.; Stack, T. D. P.; Sunderland, C. J.; Raymond, K. N. *Inorg. Chim. Acta* **1997**, *263*, 341.
(51) Manos, M. J.; Tasiopoulos, A. J.; Raptopoulou, C.; Terzis, A.; Woollins, J. D.; Slawin, A. M. Z.; Keramidas, A. D.; Kabanos, T. A. *J. Chem. Soc., Dalton Trans.* **2001**, 1556.
(52) Barauh, B.; Chakravorty, A. *Indian J. Chem., Sect. A: Inorg., Bioinorg., Phys., Theor. Anal. Chem.* **2003**, *42*, 2677.
(53) Maurya, M. R.; Agarwal, S.; Abid, M.; Azam, A.; Bader, C.; Ebel, M.; Rehder, D. *Dalton Trans.* **2006**, 937−947.

(54) According to TDDFT computations at the B3LYP/AE1+ level, the lowest excited state in **9** (at λ = 720 nm) can to a large extent be described as a HOMO−LUMO transition. Despite the known deficiencies of TDDFT for charge-transfer states (see, e.g., Dreuw, A.; Head-Gordon, M. *J. Am. Chem. Soc.* **2004**, *126*, 4007), this number compares reasonably well to experiment, λ = 870 nm (ref 2). A much higher excitation energy, corresponding to λ = 552 nm, is predicted for the innocent complex **11**.

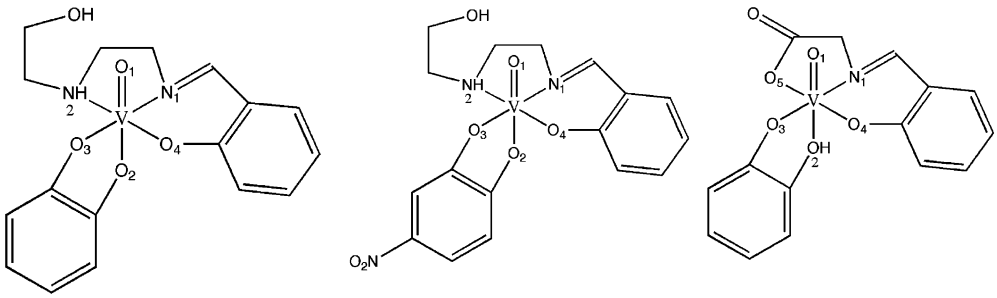

9. VO(HSHED)(CAT)[2] KUZXOS **10.** VO(HSHED)(4-NC) **11.** VO(GSAL)(HCAT)[5] XUDLIR

Figure 5. Prototypical complexes containing catechol-based ligands with variable extent of non-innocence. HSHED = (*N*-salicylideneaminato)-*N*′-(2-hydroxyethyl)ethylenediamine, GSAL = *N*-salicylideneglycinato-*N*,*O*,*O*′, CAT = catecholato, and 4-NC = 4-nitrocatecholato. Refcodes from the Cambridge Structure Database are included, where available.

Table 4. Observed and Computed Properties of **9**−**11**

property[a]	**9**	**10**	**11**
δ_{iso}(obs)	221	−194	−460
δ_{iso}	−5	−173	−587
$\delta_{11}/\delta_{22}/\delta_{33}$[b]	328/42/−307	−171/−428/−780	−294/−320/−1073
$\epsilon_{HOMO}/\epsilon_{LUMO}$ [eV][c]	−5.12/−2.88	−5.77/−3.43	−6.26/−3.43
$\Delta\epsilon_{HOMO-LUMO}$ [eV][d] (*BP*/B3LYP/**BHandH**)	*1.14*/2.23/**3.94**	*1.25*/2.34/**4.16**	*1.63*/2.83/**4.76**
ΔE_{S-T} [eV][e] (*BP*/B3LYP/**BHandH**)	*1.17*/0.48/−**0.47**	*1.40*/0.78/−**0.10**	1.89/1.47/**0.75**
closed-shell stable[f] (*BP*/B3LYP/**BHandH**)	*yes*/no/**no**	*yes*/no/**no**	*yes*/yes/**yes**

[a] Computed data in normal face are obtained for BP86/AE1-optimized geometries and B3LYP/AE1+. BP/B3LYP/BHandH triples denote results obtained with BP86 (in italics), B3LYP, and Becke's half-and-half (boldface) functionals, all employed with AE1+ basis and BP86/AE1 geometries. [b] Principal components of the chemical-shift tensor (relative to the isotropic magnetic shielding of $VOCl_3$). [c] Orbital eigenvalues (MO energies). [d] HOMO−LUMO gap. [e] Singlet−triplet gap evaluated at the closed-shell singlet BP86/AE1 geometry. [f] Stability of closed-shell singlet wavefunction.

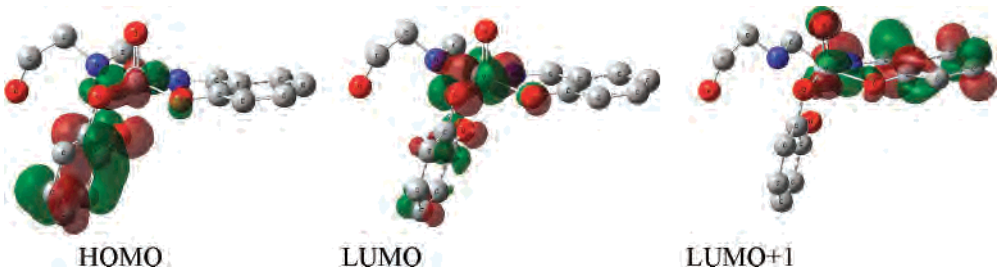

Figure 6. Frontier MOs in **9** (B3LYP/AE1+ level); H atoms omitted for clarity.

Scheme 2). The latter possibility, i.e., the occurrence of a concomitant temperature-dependent paramagnetic term arising from nonzero spin density at the metal has already been mentioned in ref 2.

A detailed investigation of all complexes in the data set from Figure 4 is well beyond the scope of this study. We have therefore selected a subset of three complexes for further scrutiny. These comprise **9**, a catecholate complex with δ_{obs} = 221 ppm, i.e., a strongly deshielded resonance well above 100 ppm, its nitro derivative **10** with δ_{obs} = −173 ppm, i.e., deshielded, but well below 100 ppm, and **11**, a monoionized catecholate complex (or aromatic ester) with δ_{obs} = −460 ppm, i.e., only slightly deshielded from the usual vanadate range.[55] Complexes **9** and **11** have been additionally characterized via X-ray crystallography.[2,5] The nitro derivative **10** has been taken to be isostructural to **9** (see Table S5, Suppporting Information, for geometrical parameters). The first of the two major structural features that differ between **9** and **11** is that of the protonation state of the catechol ligand and the second is that of the O,O′,N vs O,N,N′ binding motifs of the tridentate co-ligands. The complexes are sketched in Figure 5, and the salient DFT results are reported in Table 4.

Breakdown of the isotropic ^{51}V chemical shift into the principal components shows that there are noticeable anisotropies in all cases and that the observed decrease in δ_{iso} on going from **9** to **11** is due to a more or less equal increase in shielding along all three axes, not just along one. This is an indication that it is not a single magnetic coupling within a pair of occupied and virtual MOs that is responsible for the observed trends in δ_{iso}. For **9**, the direction of strongest deshielding roughly coincides with the V−O axis involving the O atom of the salicylideneaminato ligand. Inspection of the frontier MOs (Figure 6) reveals that the highest-occupied MO (HOMO) is largely located on the catechol moiety with significant contribution from a d orbital on vanadium and that the lowest-unoccupied MO (LUMO) is essentially made up from the same d orbital on the metal. Magnetic coupling of these MOs will thus be very weak, as the magnetic

(55) We have also looked at other systems related to **9** and **11** that contained different tridendate ligands and/or alkyl-substituted catechols and which afforded results very similar to the ones reported here.

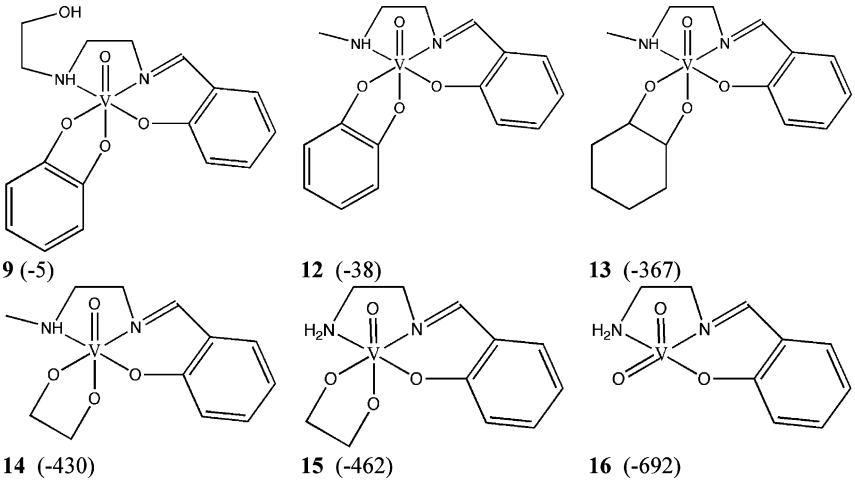

Figure 7. A series of model complexes of **9**, together with computed gas-phase equilibrium ^{51}V chemical shifts (GIAO-B3LYP/AE1+ level, in parentheses).

(angular momentum) operator acting on a d orbital will "rotate" it into another d orbital[56] with little overlap with the first one. Hence, only small paramagnetic contributions are to be expected due to this MO pair. The next-highest virtual MO, on the other hand, has large contributions from another d orbital on vanadium, namely, one which is involved in $d_\pi - p_\pi$*-type antibonding interaction with the terminal oxo ligand. Upon action of the magnetic operator on the HOMO along the direction of the strongest deshielding, the correspondingly transformed MO can mix with the LUMO+1, consistent with large paramagnetic contributions and, hence, a strong deshielding in that direction. The fact that the HOMO and LUMO+1 orbitals have large contributions from the catechol and salicylideneaminato ligands, respectively, is consistent with the observation that it is not only the non-innocent bidentate ligand that affects the ^{51}V chemical shift but also the other tridentate Schiff base.[2]

A detailed analysis of all possible, magnetically allowed MO couplings is rather cumbersome. We just note that the frontier MOs depicted in Figure 6 for **9** are qualitatively the same for **10** and **11**, as well. On going from **9** to **11**, the energetic separation of these MOs increases notably (cf. the HOMO−LUMO gap $\Delta\epsilon$ in Table 4, the HOMO−LUMO+1 gap increases similarly), consistent with decreased paramagnetic contributions in that series and, thus, with the observed and computed trends in δ_{iso}. In addition, the HOMOs of **10** and **11** have a somewhat lower metal-d contribution than that of **9** (the sum of the squared d−AO coefficients in these MOs are 0.10, 0.02, and 0.04 in **9**, **10**, and **11**, respectively), suggesting reduced overlap of the corresponding coupled MOs in **10** and **11** and, thus, a further decrease of paramagnetic contributions. In **11**, the paramagnetic contributions are apparently reduced to such an extent that they are not much different from those in normal vanadates, essentially depriving the monoionized catechol ligand of non-innocent character. In oxidized amavadin **2a**, the B3LYP wavefunction is stable and is characterized by even larger $\Delta\epsilon_{HOMO-LUMO}$ and ΔE_{S-T} values (3.75 and 1.97 eV, respectively) than in **11**, further corroborating the innocent nature of the ligands in amavadin.

Table 5. Observed and BP86/AE1-Optimized Bond Lengths (Å) of the Vanadium Catecholate **9** and Its Model Complexes

	9 expt[a]	**9**	**12**	**13**	**14**	**15**	**16**
V=O_1	1.607	1.620	1.618	1.638	1.632	1.634	1.632
V−O_2^{ax}	2.154	2.119	2.146	2.021	2.018	2.009	
V−O_3^{eq}	1.888	1.873	1.869	1.834	1.832	1.834	1.630[b]
V−O_4^{eq}	1.892	1.919	1.911	1.831	1.893	1.892	1.928
V−N_1	2.115	2.132	2.137	2.221	2.156	2.159	2.183
V−N_2	2.192	2.258	2.223	2.336	2.278	2.248	2.212

[a] Solid state, from ref 2. [b] V=O bond.

In an analogous fashion to the earlier section on amavadin, we now investigate possible substituent effects via successive cleavage of the ligands in **9** (see Figure 7). As expected, the $\delta(^{51}V)$ value shows only a very small change when the dangling hydroxyethyl group is clipped (compare **9** with **12** in Figure 7). Saturation of the catechol ligand, on the other hand, does show a very large effect, with a predicted shielding of the metal by more than 300 ppm (compare **12** with **13**). This is what we would ascribe to the non-innocent nature of the catechol ligand, excluding temperature-dependent paramagnetic contributions (see below).

The vanadium nucleus in model species **13** is still noticeably deshielded with respect to normal vanadates. Part of this deshielding may originate from the steric effects of the bulky cyclohexyl moiety, which induces some elongations of the V−N bonds with the tridentate ligand, by as much as 0.11 Å (compare the last two entries for **12** and **13** in Table 5). Replacing the cyclohexyl moiety with a simple ethylene bridge (cf. **14**) roughly restores the vanadium−ligand distances as found in **12**, thereby affording a further slight shielding of the metal. If taken as the difference in $\delta(^{51}V)$ between **12** and **14**, the non-innocence of the catechol ligand would amount to ca. 400 ppm. Probing the additional effect of an alkyl group at a coordinated N atom (cf. **14** vs **15**) or that of two alkoxy groups vs one oxo group (**15** vs **16**) produces changes in the ^{51}V chemical shift that are entirely compatible with the corresponding changes in the

(56) For pictorial rationalizations of such paramagnetic contributions in transition-metal complexes see, e.g.: (a) Berger, S.; Bock, W.; Frenking, G.; Jonas, V.; Müller, V. *J. Am. Chem. Soc.* **1995**, *117*, 3820. (b) Ruiz-Morales, Y.; Ziegler, T. *J. Phys. Chem. A* **1998**, *102*, 3970. Unfortunately, the *Gaussian* program employed in the present study does not allow for a detailed analysis of such individual MO contributions.

amavadin models (cf. **5**−**8** in Figure 2). The $\delta(^{51}V)$ value predicted for model **16** can be compared to the observed resonance at $\delta = -529$ for VO_2(HSHED),[2] revealing the usual overestimation of the metal shielding in vanadates at the DFT level employed.

Spin States. We now briefly address the question of the importance of vanadium(IV)−semiquinone configurations (cf. Scheme 2). Unfortunately, accurate computation of energetics pertaining to different spin states is a notorious problem for present-day DFT.[57] For instance, the relative energies of close-lying states can be very sensitive to the chosen functional, often critically depending on the amount of Hartree−Fock (HF) exchange that is included.[58]

In complexes **9**−**11**, an LMCT corresponding to the situation in Scheme 2 can be enforced by computing the triplet state. At all levels (and concentrating on vertical transitions at the restricted singlet geometry), these triplet states are characterized by expectation values $\langle S^2 \rangle$ around 2 and by spin densities of ca. 1 both on vanadium and on the catecholate unit as a whole. As expected, the singlet−triplet gap is strongly dependent on the functional, as exemplified by the BP86, B3LYP, and BHandH data in Table 4, which incorporates, respectively, 0, 20, and 50% of HF exchange. Even though the inclusion of HF exchange successively increases the HOMO−LUMO gap, it causes the singlet−triplet splitting to decrease spectacularly, to the extent that the triplet becomes even more stable than the singlet at the BHandH level for **9** and **10**. It is difficult to gauge which of the functionals is most accurate in the present cases. For a number of iron-based spin-crossover systems, the inclusion of 15% HF exchange has been found beneficial[58] (which would lead to results intermediate between the BP and B3LYP data in Table 4),[59] but it is unclear without extensive validation if that would hold true for the vanadium complexes of this study as well.[60]

When performing a stability check,[40] the restricted closed-shell singlet wavefunctions turned out to be unstable for **9** and **10** when HF exchange is incorporated. Indeed, at the UB3LYP level we could locate a broken-symmetry (BS) solution for an open-shell singlet state of **9**, which is slightly lower in energy (by ca. 1.5 kcal/mol) than the restricted closed-shell determinant.[61] In this BS state, which is significantly spin-contaminated with $\langle S^2 \rangle = 0.41$, a significant spin density around 0.7 is localized on the metal (and with opposite sign, mainly on the catecholate).

In view of the strong functional-dependence of the results, it is difficult to draw definite conclusions from them. What appears to be clear at this point is that complex **11** with its innocent ligand has a normal closed-shell ground state (stable wavefunction and significant singlet−triplet splitting throughout). Complexes **10** and, in particular **9**, are indicated to have a more complicated electronic structure. It is certainly possible that they have some open-shell character, in either the form of an open-shell singlet ground state or via thermally accessible triplet states. As the latter would entail a huge spin density on the metal, they would probably have to be populated only to a small extent to produce large effects on the observed ^{51}V chemical shifts.[62] The computation of NMR properties for open-shell species has recently become possible,[63,64] and non-innocent complexes of the type studied here could be an interesting target for this type of calculations.

In view of the rather good performance of the restricted B3LYP method for the ^{51}V chemical shift of **10**, we favor the interpretation that in this and related cases (cf. the points in the upper left of Figure 4) the systems can be reasonably well described by a closed-shell singlet wavefunction[65] and that additional deshieldings (as in the data in the lower right of Figure 4) are due to a temperature-dependent paramagnetic term, possibly arising from the thermal population of paramagnetic states.

Conclusions

We have computed and analyzed ^{51}V chemical shifts of two families of compounds, oxidized amavadin derivatives and vanadium catecholate complexes, both of which appear in unusually deshielded regions of the ^{51}V chemical-shift scale. For the oxidized amavadin systems, this deshielding can be broken down into a number of increments from regular substituent effects, the most important of which

(57) See for example: Ghosh, A. *J. Biol. Inorg. Chem.* **2006**, *11*, 712 and references therein.

(58) (a) Reiher, M.; Salomon, O.; Hess, B. A. *Theor. Chem. Acc.* **2001**, *107*, 48. (b) Reiher, M. *Inorg. Chem.* **2002**, *41*, 6928.

(59) For the computation of the EPR parameters of vanadium(IV) complexes, on the other hand, the use of a hybrid functional with 50% HF exchange is beneficial (see, e.g., ref 17, and: Munzarova, M. L.; Kaupp, M. *J. Phys. Chem. B* **2001**, *105*, 12644). For ^{51}V chemical shifts of vanadium complexes, the use of the BHandH functional typically leads to a deshielding with respect to the B3LYP values; while this brings the computed $\delta(^{51}V)$ value of, e.g., **9**, closer to experiment, the overall performance for a larger set of normal vanadium complexes deteriorates significantly (Geethalakshmi, K. R.; Bühl, M. unpublished results).

(60) Such an extensive validation is beyond the scope of this study. In context with the catechol complexes scrutinized here, we verified that one of the more deshielded compounds included in Figure 5 (VO(SALIMH)DBC with $\delta_{obs} = 600$ ppm, cf. entry 2 in Table S4 in the Supporting Information) still has a singlet ground state at the B3LYP level (the ΔE_{S-T} values (in eV) are *+1.14*/+0.34/**−0.63** at *BP*/B3LYP/**BHandH**, respectively, i.e., somewhat lower than those of compound **9** in Table 4). If a triplet ground state would have been predicted with B3LYP (erroneously, because the ^{51}V NMR spectrum can be recorded), then the amount of HF exchange would certainly have to be reduced below the 20% contained in the standard version of this functional, down to a value at which a singlet ground state would be obtained.

(61) Even though such single-reference BS solutions do not provide an appropriate description of the true open-shell wavefunction, they can be used to estimate magnetic exchange couplings in transition-metal complexes, cf: (a) Noodleman, L. *J. Chem. Phys.* **1981**, *74*, 5737. For a recent review see: (b) Ciofini, I.; Daul, C. *Coord. Chem. Rev.* **2003**, *238*−*239*, 187.

(62) In that case, the observed resonances should shift strongly with temperature. To our knowledge, no such temperature-dependent NMR studies have been performed yet for the complexes in question. Admixture of paramagnetic states should also lead to substantial line broadening, and indeed, very broad lines (half-width 2−4 kHz) have been reported for some of the catchol complexes in ref 2.

(63) Moon, S.; Patchkovskii, S. In *Calculation of NMR and EPR Parameters. Theory and Applications*; Kaupp, M.; Bühl, M.; Malkin, V. G., Eds.; Wiley-VCH: Weinheim, Germany, 2004; p 325.

(64) Hrobarik, P.; Reviakine, R.; Arbuznikov, A. V.; Malkina, O. L.; Malkin, V. G.; Köhler, F. H.; Kaupp, M. *J. Chem. Phys.* **2007**, *126*, 024107.

(65) It cannot be excluded, however, that the good performance of the restricted B3LYP method in systems with an unstable closed-shell wavefunction is to some extent fortuitous.

arising from the non-oxo nature of these complexes. $\delta(^{51}V)$ values computed for static equilibrium geometries show only little variation for diastereomeric isomers. The observed noticeable discrimination in the case of diastereomeric mixtures is indicated to be dynamic in origin. Even though chemical shifts averaged over MD trajectories apparently can reproduce certain experimental trends, the definite assignment of individual ^{51}V resonances to specific isomers is difficult at this point.

According to chemical-shift computations for a typical vanadium−catecholate complex and the smaller models derived thereof, the low-lying LMCT state involving catechol ligand and metal accounts for ca. 300−400 ppm of the deshielding of the ^{51}V nucleus in the closed-shell singlet wavefunction. This part of the non-innocence is indicated to originate from regular temperature-independent paramagnetic contributions and is reasonably well captured with the standard computational approach for a larger set of complexes with total ^{51}V chemical shifts of up to ca. 100 ppm. Electron-withdrawing substituents on the catecholate moiety can reduce the non-innocent character significantly (e.g., by attaching a nitro group to the aromatic ring) or quench it almost fully (e.g., by protonating one of the O donors).

Observed $\delta(^{51}V)$ values exceeding this value around 100 ppm tend to be significantly underestimated in the computations. We propose that in such cases the non-innocence of the ligands manifests itself in additional temperature-dependent paramagnetic contributions due to a noticeable open-shell character of the wavefunctions and/or thermal population of triplet states. The inherent shortcomings of present-day approximate DFT, unfortunately, currently prevent definite conclusions concerning such spin states, inviting further scrutiny with appropriate methods based, e.g., on a multiconfigurational ansatz.[66]

With these potential shortcomings borne in mind, standard DFT methods for the computation of NMR properties can still be applied to a large number of vanadium complexes with non-innocent ligands, providing a means for interpretation, at least qualitatively, of observed trends in the ^{51}V chemical shifts.

Acknowledgment. This work was supported by the Deutsche Forschungsgemeinschaft. M.B. also wishes to thank Prof. Walter Thiel and the Max-Planck Society for support and Prof. M. Kaupp for helpful discussions. Computations were performed on a local computer cluster of Intel Xeon and Opteron workstations and PCs at the MPI Mülheim facility maintained by Horst Lenk.

Supporting Information Available: Additional tabular and graphical material pertaining to geometrical parameters and NMR properties of compounds **2**, **7**−**11**, and the full set of complexes of Figure 4. This material is available free of charge via the Internet at http://pubs.acs.org.

IC701650Y

(66) See for instance: Grimme, S.; Waletzke, M. *J. Chem. Phys.* **1999**, *111*, 5645.